Versatile large-mode-area femtosecond laser-written Tm:ZBLAN glass chip lasers

D. G. Lancaster,[1,*] S. Gross,[2] A. Fuerbach,[2] H. Ebendorff Heidepriem,[1] T. M. Monro,[1] and M. J. Withford[2]

[1] IPAS and School of Chemistry & Physics, University of Adelaide, South Australia, 5005, Australia
[2] Centre for Ultrahigh-bandwidth Devices for Optical Systems (CUDOS) and MQ Photonics Research Centre, Department of Physics and Astronomy, Macquarie University, New South Wales 2109, Australia
[*]david.lancaster@adelaide.edu.au

Abstract: We report performance characteristics of a thulium doped ZBLAN waveguide laser that supports the largest fundamental modes reported in a rare-earth doped planar waveguide laser (to the best of our knowledge). The high mode quality of waveguides up to 45 um diameter (~1075 μm^2 mode-field area) is validated by a measured beam quality of M^2~1.1 ± 0.1. Benefits of these large mode-areas are demonstrated by achieving 1.9 kW peak-power output Q-switched pulses. The 1.89 μm free-running cw laser produces 205 mW and achieves a 67% internal slope efficiency corresponding to a quantum efficiency of 161%. The 9 mm long planar chip developed for concept demonstration is rapidly fabricated by single-step optical processing, contains 15 depressed-cladding waveguides, and can operate in semi-monolithic or external cavity laser configurations.

OCIS codes: (140.3070) Infrared and far-infrared lasers; (140.3580) Lasers, solid-state; (140.3390) Laser materials processing; (230.7380) Waveguides, channeled.

References and links

1. S. Taccheo, G. D. Valle, R. Osellame, G. Cerullo, N. Chiodo, P. Laporta, O. Svelto, A. Killi, U. Morgner, M. Lederer, and D. Kopf, "Er:Yb-doped waveguide laser fabricated by femtosecond laser pulses," Opt. Lett. **29**(22), 2626–2628 (2004).
2. M. Ams, G. D. Marshall, P. Dekker, J. A. Piper, and M. J. Withford, "Ultrafast laser written active devices," Laser & Photon. Rev. **3**(6), 535–544 (2009).
3. T. Calmano, J. Siebenmorgen, O. Hellmig, K. Petermann, and G. Huber, "Low loss depressed cladding waveguide inscribed in YAG: Nd single crystal by femtosecond laser pulses," Appl. Phys. B **100**, 131–135 (2010).
4. C. Grivas, "Optically pumped planar waveguide lasers, Part I: Fundamentals and fabrication techniques," IEEE Prog. Quantum Electron. **35**(6), 159–239 (2011).
5. J. D. Musgraves, K. Richardson, and J. Jain, "Laser-induced structural modification, its mechanisms, and applications in glassy optical materials," Opt. Mater. Express **1**(5), 921–935 (2011).
6. X. Zhu and N. Peyghambarian, "High power ZBLAN fiber lasers: review and prospect," Adv. Optoelectron. **2010**, 501956 (2010).
7. L. Wetenkamp, G. F. West, and H. Tobben, "Optical properties of rare earth-doped ZBLAN glasses," J. Non-Cryst. Solids **140**, 35–40 (1992).
8. R. Paschotta, N. Moore, W. A. Clarkson, A. C. Tropper, D. C. Hanna, and G. Maze, "230 mW of blue light from a thulium-doped upconversion fiber laser," IEEE J. Sel. Top. Quantum Electron. **3**(4), 1100–1102 (1997).
9. S. Tokita, M. Murakami, S. Shimizu, M. Hashida, and S. Sakabe, "Liquid-cooled 24 W mid-infrared Er:ZBLAN fiber laser," Opt. Lett. **34**(20), 3062–3064 (2009).
10. J. Schneider, C. Carbonnier, and U. B. Unrau, "Characterization of a Ho^{3+}-doped fluoride fiber laser with a 3.9-μm emission wavelength," Appl. Opt. **36**(33), 8595–8600 (1997).
11. D. C. Tran, G. H. Sigel, and B. Bendow, "Heavy metal fluoride glasses and fibers: A review," J. Lightwave Technol. **2**(5), 566–586 (1984).
12. S. F. Carter, M. W. Moore, D. Szebesta, J. R. Williams, D. Ranson, and P. W. France, "Low loss fluoride fiber by reduced pressure casting," Electron. Lett. **26**(25), 2115–2117 (1990).
13. W. A. Gambling, "The rise and rise of optical fibers," IEEE J. Sel. Top. Quantum Electron. **6**(6), 1084–1093 (2000).

14. J. L. Adam, F. Smektala, and J. Lucas, “Active fluoride glass optical waveguides for laser sources,” Opt. Mater. **4**(1), 85–90 (1994).
15. J. Colaizzi and M. J. Matthewson, “Mechanical durability of ZBLAN and aluminum fluoride-based optical fiber,” J. Lightwave Technol. **12**(8), 1317–1324 (1994).
16. O. Perrot, L. Guinvarc'h, D. Benhaddou, P. C. Montgomery, R. Rimet, B. Boulard, and C. Jacoboni, “Optical investigation of fluoride glass planar waveguides made by vapour phase deposition,” J. Non-Cryst. Solids **184**, 257–262 (1995).
17. J. D. Shephard, D. Furniss, P. A. Houston, and A. B. Seddon, “Fabrication of mid-infrared planar waveguides from compatible fluorozirconate glass pairs, via hot spin-casting,” J. Non-Cryst. Solids **284**(1-3), 160–167 (2001).
18. M. Waldmann, R. Caspary, D. Wortmann, J. Gottmann, and W. Kowalsky, “Erbium-doped fluoride glass waveguides,” Electron. Lett. **44**(20), 1193 (2008).
19. D. W. J. Harwood, A. Fu, E. R. Taylor, R. C. Moore, Y. D. West, and D. N. Payne, “A 1317nm neodymium doped fluoride glass waveguide laser,” ECOC 2000. 26th European Conference on Optical Communication **2**, 191–2 (2000)
20. D. G. Lancaster, S. Gross, H. Ebendorff-Heidepriem, K. Kuan, T. M. Monro, M. Ams, A. Fuerbach, and M. J. Withford, “Fifty percent internal slope efficiency femtosecond direct-written Tm^{3+}:ZBLAN waveguide laser,” Opt. Lett. **36**(9), 1587–1589 (2011).
21. D. G. Lancaster, S. Gross, H. Ebendorff-Heidepriem, A. Fuerbach, M. J. Withford, and T. M. Monro, “2.1 μm waveguide laser fabricated by femtosecond laser direct-writing in Ho^{3+}, Tm^{3+}:ZBLAN glass,” Opt. Lett. **37**(6), 996–998 (2012).
22. M. Eichhorn and S. D. Jackson, “Comparative study of continuous wave Tm^{3+}-doped silica and fluoride fiber lasers,” Appl. Phys. B **90**(1), 35–41 (2008).
23. K. van Dalfsen, S. Aravazhi, C. Grivas, S. M. García-Blanco, and M. Pollnau, “Thulium channel waveguide laser in a monoclinic double tungstate with 70% slope efficiency,” Opt. Lett. **37**(5), 887–889 (2012).
24. C. Schaffer, J. Garcia, and E. Mazur, “Bulk heating of transparent materials using a high-repetition-rate femtosecond laser,” Appl. Phys., A Mater. Sci. Process. **76**(3), 351–354 (2003).
25. B. M. Walsh and N. P. Barnes, “Comparison of Tm:ZBLAN and Tm:silica fiber lasers: Spectroscopy and tunable pulsed laser operation around 1.9 μm,” Appl. Phys. B **78**(3-4), 325–333 (2004).
26. J. Hu and C. R. Menyuk, “Understanding leaky modes: slab waveguide revisited,” Adv. Opt. Photon. **1**(1), 58–106 (2009).
27. D. Findlay and R. A. Clay, “The measurement of internal losses in 4-level lasers,” Phys. Lett. **20**(3), 277–278 (1966).
28. S. D. Jackson, “High-power and highly efficient diode-cladding-pumped holmium-doped fluoride fiber laser operating at 2.94 microm,” Opt. Lett. **34**(15), 2327–2329 (2009).

1. Introduction

Since the first demonstration of a femtosecond (fs) laser to inscribe a waveguide into an actively doped material for laser application in 2004 [1], a variety of lasers in both glass and crystal hosts have been reported [2–5]. However, there has been no direct-write waveguide architecture and material combination reported that possesses an ultra-large fundamental mode-area; a critical characteristic to enable high peak-power Q-switched and mode-locking operation.

Rare-earth doped heavy metal fluoride glass fiber lasers based on ZBLAN (ZrF_4, BaF_4, LaF_4, AlF_3, NaF_3) have the distinction of being the most spectrally diverse fiber lasers as they can support laser operation from the visible [6–8] through to 3.9 μm [9,10]. As a laser host material ZBLAN is without peer due to the combination of wide transparency from the UV through to 5 μm [11], a low phonon energy of 550 cm^{-1} [7] and a high rare-earth (RE) solubility resulting in high-gain per unit length. This combination of properties are the result of weak ionic bonding, and a composition containing heavy metal ions which leads to low resonance frequencies of this glass. RE doped low phonon energy glasses are essential for mid-infrared and upconversion lasers as they have reduced phonon assisted decay from upper laser-levels and possess long excited-state lifetimes which additionally aids efficient infrared pump upconversion into the visible.

Although ZBLAN fiber lasers were heavily developed during the latter part of the last century due to the aforementioned advantages and predicted lower bulk losses compared to silica fiber lasers [12,13], these performance advantages were never fully capitalized. While rare-earth doped ZBLAN fiber lasers are still the highest power solid-state lasers in the 2.3 –

#176801 - $15.00 USD Received 25 Sep 2012; accepted 4 Nov 2012; published 27 Nov 2012

3.9 μm spectral region with 24 W achieved at 2.7 μm [9], their transition outside the laboratory has been hampered by handling and splicing difficulties, lack of ZBLAN fiber components, critical packaging requirements, and the high cost of manufacturing ZBLAN fibers.

For low-to-medium average power applications, planar waveguides are a potentially superior approach to realizing versatile ZBLAN glass lasers. In a 1994 review paper covering the potential of rare-earth doped fluoride glass optical waveguides it was stated "because of the similarities with optical fibers, in terms of light guiding and confinement, planar waveguides are expected to show laser action at most of the wavelengths listed (with reference to ZBLAN fiber lasers achieving wavelengths covering 0.455 to 3.45 μm)" [14]. In terms of device ruggedness, embedded waveguides are inherently protected from air and moisture exposure, unlike ZBLAN fibers which have large surface areas and can weaken and degrade over time unless elaborate precautions are taken [15]. Approaches investigated to fabricate waveguides in fluoride glasses involve multi-step processes such as vapor phase deposition [16], hot dip spin coating [17] and photolithography/ wet-etching [18]. The only report of a fluoride glass waveguide laser (specifically Nd^{3+} operating at 1.0 and 1.3 μm) was based on a complex fabrication procedure involving hot dip spin coating deposition of core and cladding layers, with 244 nm cw laser-writing used to achieve lateral confinement [19].

Alternatively, waveguides can be written using ultrafast laser material modification of rare-earth doped glasses and crystals [1,3]. In 2011 we were the first group to report a direct-write rapid-fabrication method to create embedded guiding channels in rare-earth doped ZBLAN glass using fs laser modification [20]. We reported laser operation in these waveguides and presented preliminary slope efficiencies and spectral characteristics of a free-running Tm^{3+} doped $\lambda = 1.9$ μm ZBLAN waveguide laser. More recently we published the first Ho^{3+} ZBLAN waveguide laser which allowed the extension of the wavelength to 2.1 μm [21].

Here we report a significant advance in the development of these ZBLAN chip lasers as a versatile and highly efficient platform technology. Specifically we report characteristics of rare-earth doped ZBLAN glass waveguides and its interaction with intense MHz-rate fs laser pulses that results in the formation of depressed cladding structures that capitalize on leaky-mode designs that underpin large mode-area guidance. To illustrate the benefits of the large single transverse mode channels we show that they are ideal for high peak-power generation and utilize this characteristic by generating Q-switched pulses of up to 1.9 kW peak-power with close-to diffraction limited and symmetrical beam-quality. These waveguides possess the largest single transverse mode areas (~1075 μm^2) reported to date in a rare-earth doped waveguide laser (to the best of our knowledge). The internal cw laser slope efficiency of 67% comfortably exceeds the highest 790 nm pumped Tm^{3+} ZBLAN fiber laser efficiency of 49% reported [22], and is comparable to the 70% slope efficiency reported for a liquid phase epitaxy grown heavily thulium-doped double-tungstate crystal waveguide laser [23].

2. Experiments and results

To inscribe the waveguides in ZBLAN we use a MHz repetition-rate $\lambda = 800$ nm fs laser to write modified density inclusions. We have discovered that when high repetition rate low-energy pulses (<100 nJ) are tightly focused into small volumes (~1 μm^3) of ZBLAN, a significantly larger volume of lower density glass with a symmetric shape and reduced refractive index (Δn~-1.6 × 10^{-3}) is produced [20]. By translating the sample, 'rods' of reduced refractive index can be produced. When these rods are overlapped a symmetric and configurable guiding structure (see Fig. 1(a)) is produced whereby the inscribed region can serve as a depressed cladding surrounding an unmodified core region (as illustrated in the plot of refractive index as a function of radius in Fig. 1(a)). Each individual circular rod is formed due to isotropic heat diffusion where the energy of multiple pulses is deposited within the

#176801 - $15.00 USD Received 25 Sep 2012; accepted 4 Nov 2012; published 27 Nov 2012

thermal diffusion time which leads to a cumulative heating effect [24]. In the device considered in this work, 24 low-index rods are inscribed longitudinally into the glass in a 2-ring geometry to realize different waveguide core diameters as shown schematically in Fig. 1(a). Note the cladding is built from the 'bottom up' such that previously irradiated regions are not written through.

The ZBLAN glass was fabricated in-house (using commercially available raw materials) in a controlled atmosphere glass melting facility to create 50 g glass ingots doped with 3.7 × 10^{26} ions/m^3 of Tm^{3+} to allow efficient 2 for 1 cross relaxation of the Tm^{3+} ion when pumped at 790 nm [25]. To create the waveguide substrates the ingots were diced into chips measuring ~9 mm length, 8 mm width and 2 mm height by a CNC diamond saw. The top face of each sample was polished to allow the ultrafast laser to be focused below the surface, with the waveguide axes set at a depth of 300 μm.

The waveguides were inscribed using pulses from an ultrafast Ti:sapphire oscillator (FEMTOSOURCE XL 500 – Femtolasers GmbH, 800 nm centre wavelength, 50 fs pulse duration, 5.1 MHz repetition rate), which were focused into the chip using a 1.25 NA 100 × oil immersion objective while the sample was translated using a set of computer controlled XYZ air-bearing translation stages. The chip described here is shown in Fig. 2(b), and contains fifteen waveguides separated by 450 μm with core diameters ranging from 15 to 45 μm. They were written into the doped glass with pulse energies of 80 nJ and translation speeds of 16.7 mm/s. After waveguide writing, the end faces were polished back by ~250 μm to reveal the waveguide ends (microscope end-face image of two waveguides is shown in Fig. 1(b)).

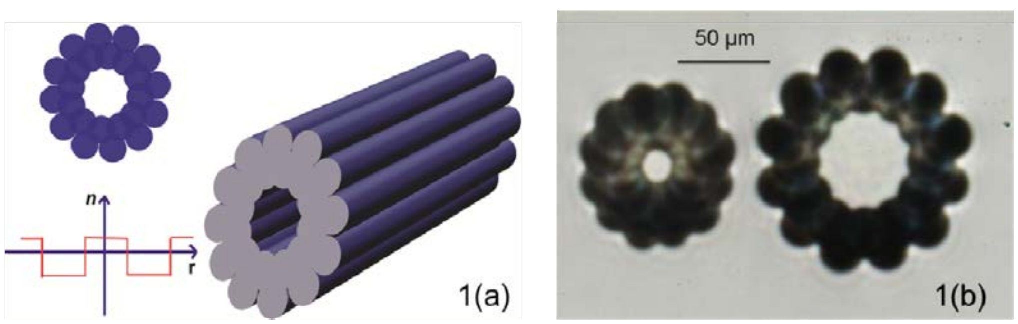

Fig. 1. (a) 2-D and 3-D representations of the depressed cladding waveguide concept; Plot of the idealized depressed cladding refractive index vs. waveguide radius. (b) Microscope image (bottom illumination) of two depressed-cladding waveguides written into thulium doped ZBLAN glass (15 & 45 μm diameters). Each waveguide has a cladding formed by 24 overlapping rods written using 80 nJ pulses (λ = 800 nm), 5.1 MHz repetition rate, 16.7 mm/s translation speed.

Figure 2(a) shows the modeling predictions for the exact EM solution for an idealized depressed cladding waveguide (also known as a 'W' or 'leaky mode' waveguide [26]), as plotted in the graph in Fig. 1(a). The predicted fundamental-mode confinement loss and first high-order mode (HOM) loss at λ = 1.9 μm are plotted as a function of waveguide core-radius for $\Delta n = -1.6 \times 10^{-3}$ and a depressed cladding region width of 22.5 μm (representative of the 2-ring structure presented in this paper). With reference to the 22.5 μm core-radius waveguide modal loss plotted in Fig. 2(a), the 1st HOM loss at 8×10^{-3} dB/cm is an order of magnitude greater than the fundamental mode (FM) loss of 6.8×10^{-4}. In essence the HOM is leakier than the FM as the peak field for the HOM is radially offset from the waveguide centre and hence penetrates further into the narrow inner cladding region. This mode discrimination ensures that the FM reaches threshold first, and suppresses the next mode. In effect this waveguide acts as a modal filter allowing a low loss fundamental laser mode to build up,

#176801 - $15.00 USD
Received 25 Sep 2012; accepted 4 Nov 2012; published 27 Nov 2012

while a combination of gain depletion, higher order mode confinement loss, and ground state absorption outside the pumped core suppress the HOMs.

To demonstrate end-pumped laser configurations the pump-end of the waveguide (shown in Fig. 3(a)) is coated with a dielectric film that is highly reflecting (HR) at the laser wavelength (λ_l~1.75-2.1 μm) and highly transmitting (HT) at λ_p = 790 nm. The other end is anti-reflection (AR) coated for λ_l and λ_p thus allowing either a semi-monolithic cavity to be used, or an extended cavity. The semi-monolithic cavity is achieved by butting up an output-coupler (OC) mirror to the chip. We note that the dielectric coatings on the waveguide end-faces have the added advantage of protecting the ZBLAN glass from long-term atmospheric exposure. To pump the Tm^{3+} doped waveguide laser up to 600 mW of CW Ti:sapphire laser light tuned to 790 nm was focused into the waveguide using a f = 50 mm lens giving a spot size of ~29 μm.

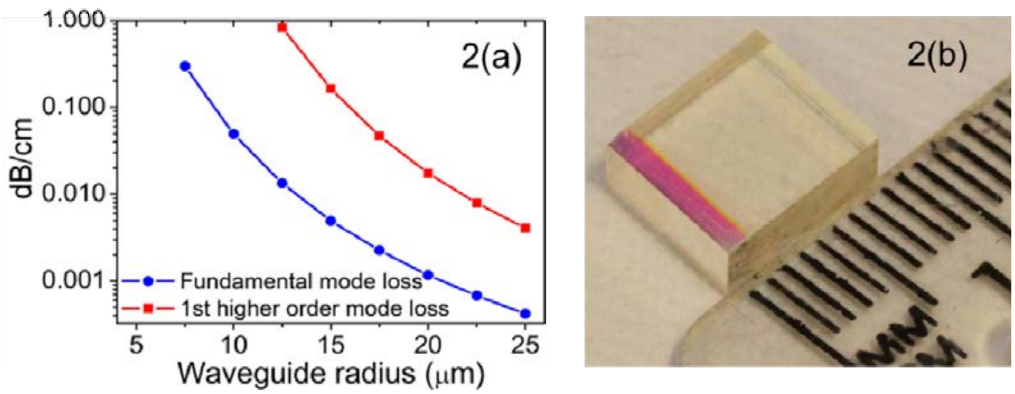

Fig. 2. (a) Predicted confinement loss of the fundamental and first higher order mode at λ = 1.9 μm for a depressed cladding waveguide as a function of waveguide core-radius. (b) Tm:ZBLAN chip containing 15 waveguides with dielectrically-coated end faces.

To determine the optimum laser slope efficiency, measurements were conducted using a range of OC mirrors, with the experimental configuration shown in Fig. 3(a). The internal laser slope efficiencies are plotted in Fig. 3(b), with the best result of 67% and 205 mW of power achieved (pump-power limited) at a threshold of 12 mW using a waveguide with a core diameter of 34 μm and a R_{OC} = 79%. Under these spectrally free-running conditions the laser operated at λ_l = 1880 nm, with a broad ~5 nm bandwidth. The chip laser loss was estimated at 0.4 ± 0.2 dB/cm by conducting a Findlay Clay [27] analysis of the measured laser thresholds as a function of output-coupling. This measured loss is notably higher than the 0.003 dB/cm confinement loss predicted for an ideal depressed clad structure (Fig. 2(a)); however determining the relative contributions of the residual Tm^{3+} ground state absorption (due to the 3-level laser transition), intrinsic glass absorption (<0.02 dB/cm), and waveguide loss, is not possible without further measurements. The waveguide loss mechanisms include scattering due to variations in the density of the cladding, deviations in the cladding shape that distort the circular symmetry, as well as waveguide wall roughness. From this measurement it is clear that further work to quantify these loss mechanisms in a direct measurement will need be undertaken. We note that this estimated loss is higher than the 0.22 dB/cm loss we reported in [20], which was incorrect, and in fact should have been 0.22 cm^{-1} (loss in [20] was dominated by uncoated WG face losses in the resonator).

#176801 - $15.00 USD Received 25 Sep 2012; accepted 4 Nov 2012; published 27 Nov 2012

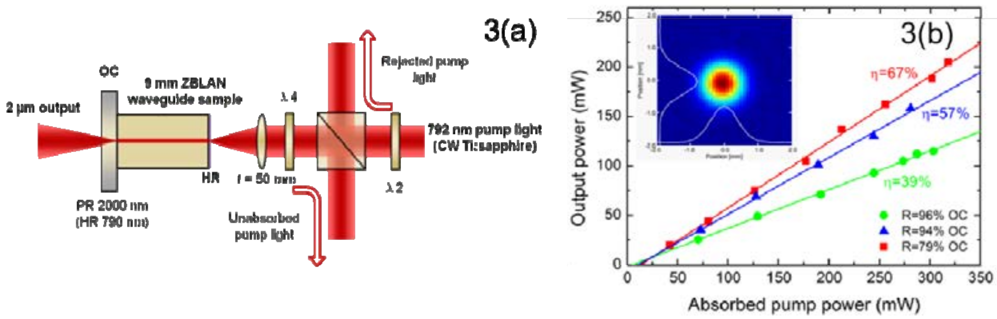

Fig. 3. (a) Experimental laser configuration for a semi-monolithic cavity made up of the waveguide chip and an external ‘butted’ discrete output-coupler mirror. (b) Measured laser slope-efficiency for the semi-monolithic waveguide laser in Fig. 3(a). Inset is the collimated output beam profile.

A key feature of a depressed cladding waveguide is that the diffraction limited ‘Gaussian-like’ FM still operates at very large core sizes due to differential higher-order mode loss. To validate fundamental mode operation for a range of waveguide diameters, the beam quality (M^2, or times diffraction limit) for the semi-monolithic configured waveguide lasers was measured. The beam quality of the chip laser was measured by focusing the laser output with a f = 1 m plano-convex lens, and recording the beam image throughout the focal region with a pyro-electric array (Spiricon Pyrocam III).

An image of the collimated output beam profile of the largest waveguide (45 µm core diameter) is shown as an inset in Fig. 3(b) with the Gaussian line shape of the beam confirming lowest order transverse mode operation. The measured M^2 values for a subset of waveguides with diameters ranging from 15 to 45 µm are shown in Fig. 4(a). The M^2 values for the 15 µm and 45 µm diameter waveguides are 1.2 ± 0.1 and 1.1 ± 0.1, respectively, again consistent with Gaussian beam shape lowest-order mode operation.

In order to investigate high peak-power operation characteristics of this large mode-area chip laser active acousto-optic Q-switching is used not only for its convenience, but also for its ability to limit the energy stored. This is critical due to the long $^3F_4$ upper state storage lifetime of 13.7 ms in Tm:ZBLAN [25]. The Q-switching cavity used had a 9 cm cavity length, a 40 µm diameter waveguide, a R_{OC} = 79%, and configured for single-pass pump.

The highest Q-switched average output power achieved was 104 mW with a 34% slope efficiency which produced 32 ns pulses at a 5 kHz repetition rate (efficiency was reduced due to a lossy AR coating on the AO-Q switch and the intra-cavity lens). By decreasing the repetition rate to 2.054 kHz, a stable train of 21 ns Q-switched pulses could be produced, corresponding to 1.85 kW peak power. Figure 4(b) shows the experimentally obtained Q-switched pulse-width and peak-power as a function of repetition rate. Figure 4(b) (inset) shows a recorded 21 ns pulse for the chip laser operating at 2.054 kHz. The AO Q-switch used for this investigation had a 15 ns decay-time and we would expect this high-gain and low cavity-lifetime configuration (1.3 ns cavity lifetime) to produce shorter pulses from a faster (possibly electro-optic) Q-switch.

3. Discussion and conclusion

While in the work described thus far we have reported the performance of this laser chip using Ti:sapphire laser pumping, we note that this pump source is not practical for most applications. To that end we have also demonstrated, for the first time, the use of compact 790 nm diode lasers to pump the semi-monolithic configured cavity using low-cost commercially available 100 mW single emitter diode-lasers. When diode-laser pumped we measured an internal slope efficiency of 40%, and up to 25 mW of light at ~1.9 µm was generated.

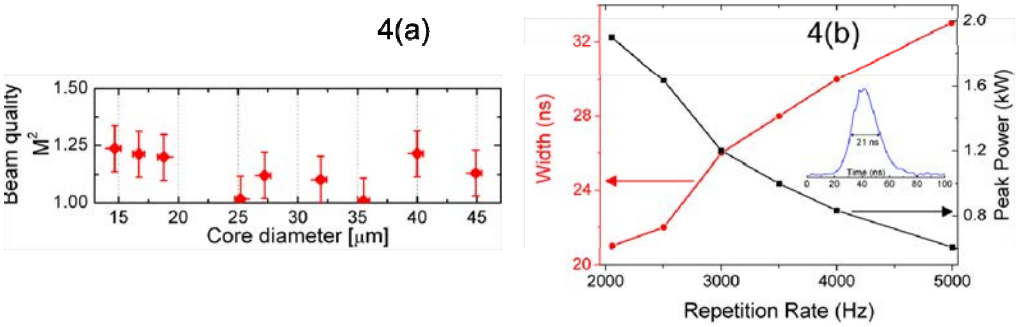

Fig. 4. (a) Measured mode quality (M^2) as a function of waveguide core diameter for the semi-monolithic cavity (b) Experimentally obtained Tm-waveguide laser Q-switching performance using an AO Q-switch in an external cavity. Inset: Representative pulse of τ = 21 ns (FWHM) obtained for at a repetition rate of 2.053 kHz, and E = 38 μJ.

Prospects are good that this waveguide device architecture and rare-earth doped ZBLAN glass combination will be capable of generating mid-infrared laser light via direct transitions; a claim supported by our high 67% internal slope efficiency. Candidate transitions demonstrated in ZBLAN fiber lasers include: an 1150 nm diode laser pumped ~3 mol% holmium double-clad fiber operating at 2.86 μm [28] and a 6 mol% erbium doped double-clad fiber operating at 2.8 μm [9] when pumped at 975 nm. To support longer wavelength laser operation in the chip architecture, the waveguides require thicker cladding structures to avoid fundamental-mode confinement loss. For instance confinement loss modeling predicts that 50 μm claddings will have confinement losses of 0.001 dB/cm at 2.9 μm, which can easily be realized by adding a third ring of cladding rods to the waveguide structure.

In conclusion we report (to the best of our knowledge) the largest fundamental mode-area rare-earth doped planar waveguide laser. The unique depressed cladding waveguide is inscribed via a reduced refractive index material modification that ZBLAN undergoes when irradiated by intense MHz-rate fs pulses. By exploiting these large mode areas up to 1.9 kW of peak-power Q-switched output are produced, thus demonstrating the potential of this architecture for operating regimes requiring high peak-power such as Q-switching and mode-locking. We have also reported an internal slope efficiency of 67% (λ_l = 1.9 μm) when pumped at 790 nm, which corresponds to a quantum efficiency of 161%. These performance characteristics coupled with the wide transmission and low phonon-energy of ZBLAN suggests that this versatile architecture has the potential to deliver the visible to mid-infrared spectral coverage of ZBLAN fiber lasers but in a compact and high efficiency, rapidly-manufacturable waveguide form-factor.

Acknowledgments

Part of this research was conducted by the Australian Research Council Centre of Excellence for Ultrahigh Bandwidth Devices for Optical Systems (project number CE110001018) and supported by Linkage Infrastructure, Equipment and Facilities programs. T. Monro acknowledges the support of an ARC Federation Fellowship. The authors appreciate assistance from Kenton Knight for providing the doped ZBLAN glass used in these experiments. Technical drawing and drafting support was provided by Alastair Dowler. Derek Abbot and Benjamin Ung contributed the laboratory and Ti:sapphire laser used for these experiments. This work was performed in part at the OptoFab node of the Australian National Fabrication Facility utilizing Commonwealth and SA State Government funding.

Optics Express

BACK TO RESULTS

Click for Open Access

Basic Description | Other Editions/ Formats | Abstracting/ Indexing & Article Access | Publisher & Ordering Information | Advertising, Rights, Demographics | Reviews

JCR Web

Click highlighted text for a new search on that item.

ISSN:	1094-4087
Title:	Optics Express
Publishing Body:	Optical Society of America
Country:	United States
Status:	Active
Start Year:	1997
Frequency:	Bi-weekly
Document Type:	Journal; Academic/Scholarly
Refereed:	Yes
Abstracted/Indexed:	Yes
Media:	Online - full content
Language:	Text in English
Price:	Free (effective 2010)
Subject:	PHYSICS - OPTICS
Dewey #:	621.36
LC#:	QC350
CODEN:	OPEXFF
Editor(s):	Martijn de de Sterke (Editor-in-Chief), Sharon Jeffress (Managing Editor)
E-Mail:	opex@osa.org
URL:	http://www.opticsinfobase.org/oe/journal/oe/about.cfm
Description:	Covers original research in optical science and technology.

Additional Title Information

ADDITIONAL TITLE INFORMATION

Alternate Title:	Medline Abbreviated title: Opt Express

Back to Top

Back to Top